exactly 1 gallium vertex of another polyhedron. The Ga(22)–Ga(23) distance of 2.43 Å is 0.1 Å shorter than the next shortest Ga–Ga distance (Ga(4)–Ga(13) = 2.53 Å), which when coupled with the lack of exopolyhedral bonds from Ga(22) and Ga(23) suggests a Ga(22)=Ga(23) double bond. If this is the case, the closed-shell electronic configuration for the edge-localized gallium satellite polyhedron depicted in Figure 2 in Ga_{15}^{15-}.

Now consider the two types of Ga_{12} icosahedra in $Na_{22}Ga_{39}$. In one type of Ga_{12} icosahedron (icosahedra A in ref 28) all 12 vertices form 2-center 2-electron external bonds (Table I) to gallium vertices either of other icosahedra or of the satellite Ga_{15} polyhedron leading to the usual closed-shell electronic configuration Ga_{12}^{2-}. However, in the other type of Ga_{12} icosahedron in $Na_{22}Ga_{39}$ (icosahedra B in ref 28), 3 of the 12 vertices are not bonded to external groups, leading to the 26 skeletal electron Ga_{12}^{5-} closed-shell electronic configuration as follows:

valence electrons of 12 Ga atoms (12)(3)	36 electrons
−5 charge on Ga_{12}^{5-}	+5 electrons
required for 9/2 external 2-center 2-electron bonds: (9/2)(2)	−9 electrons
required for 3 external lone pairs: (3)(2)	−6 electrons
net electrons remaining for skeletal electrons	26 electrons

The closed-shell electronic configurations of Ga_{12}^{2-} for icosahedra A, Ga_{12}^{5-} for icosahedra B, and Ga_{15}^{15-} for the edge-localized gallium satellite polyhedron (Figure 2) lead to the observed stoichiometry $Na_{22}(Ga_{12})_2(Ga_{15}) = Na_{22}Ga_{39}$.

Summary

This paper shows how the gallium deltahedra found in the intermetallic phases of gallium and alkali metals have geometries and chemical bonding topologies similar to those found in the deltahedral borane anions $B_nH_n^{2-}$ ($6 \le n \le 12$). This suggests the possibility of preparing globally delocalized deltahedral gallane anions $Ga_nH_n^{2-}$ ($6 \le n \le 12$) if appropriate methods can be found for forming the gallium deltahedra without breaking all of the normally very labile Ga–H bonds. In addition, the observation of an apparent Ga=Ga double bond in the Ga_{15} satellite polyhedron of $Na_{22}Ga_{39}$ suggests the possibility of preparing molecular species, such as the dianions $[R_2Ga{=}GaR_2]^{2-}$ (R = bulky alkyl groups), containing Ga=Ga double bonds. Finally the occurrence of M_{12} (M = B, Ga) icosahedra in both boron and gallium compounds (e.g., $B_{12}H_{12}$ and $RbGa_7$) as well as the existence of many aluminum alloy icosahedral quasicrystalline phases[16–18] suggests a unique tendency of the elements in the B, Al, Ga, In, Tl column of the periodic table to form icosahedral clusters exhibiting 5-fold symmetry. This feature could be used to call the elements of this column of the periodic table the "icosogens" similar to the pnicogens (N, P, As, Sb, Bi), chalcogens (O, S, Se, Te, Po), halogens (F, Cl, Br, I, At), etc.

Acknowledgment. I am indebted to the U.S. Office of Naval Research for partial support of this work.

Registry No. Ga, 7440-55-3; KGa_3, 51681-98-2; $RbGa_3$, 79882-69-2; $RbGa_7$, 80261-97-8; $CsGa_7$, 86377-00-6; Li_3Ga_{14}, 82794-14-7; K_3Ga_{13}, 74486-98-9; $Na_{22}Ga_{39}$, 81741-48-2.

Contribution from the Naval Research Laboratory, Code 6120, Washington, D.C. 20375

Chemical Vapor Deposition Experiments Using New Fluorinated Acetylacetonates of Calcium, Strontium, and Barium

A. P. Purdy,*[1] A. D. Berry, R. T. Holm, M. Fatemi, and D. K. Gaskill

Received December 28, 1988

The calcium, barium, and strontium complexes of trifluoroacetylacetone (H[TFA]) and hexafluoroacetylacetone (H[HFA]) have been prepared and characterized by IR and ^1H and ^{19}F NMR spectroscopies, melting and sublimation points, elemental analysis, and mass spectroscopy. Chemical vapor deposition experiments were performed with all the HFA complexes and with $Ca[TFA]_2$. Under an oxygen atmosphere, metal fluoride films were deposited onto silicon substrates, but in the absence of oxygen, the films had a high carbon content. Films were characterized by Auger electron spectroscopy, X-ray diffraction, thickness measurements, and scanning electron microscopy.

Introduction

There has been considerable interest in recent years in the development of new precursors for the chemical vapor deposition (CVD) of inorganic materials. In general, such precursors must be volatile, have sufficient stability to transport to the deposition site, and decompose cleanly to give the desired material. Various acetylacetonate complexes of both main-group and transition metals have been used to deposit films of metals,[2] metal oxides,[3–9] and fluorides.[10] Complexes of fluorinated acetylacetone ligands such as $F_3CC(O)CH_2C(O)CH_3$ (H[TFA]) and $[F_3CC(O)]_2CH_2$ (H[HFA]) often have greater volatility than their hydrogen analogues. The complexes $Ca[TFA]_2$ and $Ba[TFA]_2$ have been reported previously,[11] and $Ba[HFA]_2$ is commercially available[12] (although no details of its synthesis have been published). A recent report[3] describes the use of $Ba[HFA]_2$ to prepare films of Y–Ba–Cu–O. The deposition of BaF_2 from $Ba[HFA]_2$ is also mentioned, but no details are given. Here we report the results of film growth experiments with the HFA and TFA complexes

(1) NRC-NRL Cooperative Research Associate.
(2) Oehr, L.; Suhr, H. *Appl. Phys. A* **1988**, *45*, 151.
(3) Shinohara, K.; Munahata, F.; Yamanaha, M. *Jpn. J. Appl. Phys.* **1988**, *27*(9), L1683.
(4) Berry, A. D.; Gaskill, D. K.; Holm, R. T.; Cukauskas, E. J.; Kaplan, R.; Henry, R. L. *Appl. Phys. Lett.* **1988**, *52*(20), 1743.
(5) Korzov, V. F.; Ibraimov, R. S.; Galkin, B. D. *Zh. Prikl. Khim.* **1969**, *42*(5), 989.
(6) Hardee, K. L.; Bard, A. J. *J. Electrochem. Soc.* **1976**, *123*, 1024.
(7) Cowher, M. E.; Sedgwick, T. O.; Landermann, J. *J. Electron. Mater.* **1974**, *3*(3), 621.
(8) Panson, A. J.; Charles, R. G.; Schmidt, D. N.; Szedon, J. R.; Machiko, G. J.; Braginski, A. I. *Appl. Phys. Lett.* **1988**, *53*(18), 1756.
(9) Zhao, J.; Dahmen, K.; Marcy, H. O.; Tongue, L. M.; Marks, T. J.; Wessels, B. W.; Kannewurf, C. R. *Appl. Phys. Lett.* **1988**, *53*(18), 1750.
(10) Joosten, P. H.; Heller, P.; Nabben, H. J. P.; van Hai, H. A. M.; Popma, T. J. A.; Haisma, J. *Appl. Opt.* **1985**, *24*(6), 2674.
(11) Bogatskii, A. V.; Chumachenko, T. K.; Suprinovich, E. S.; Derkach, A. E.; Kuz'min, V. E. *Probl. Khim. Primen. β-Diketonatov Met.* [*Mater. Vses. Semin.*], *4th* **1982**, 171; *Chem. Abstr.* **1983**, *98*, 82739.
(12) Strem Chemicals Inc.

0020-1669/89/1328-2799$01.50/0

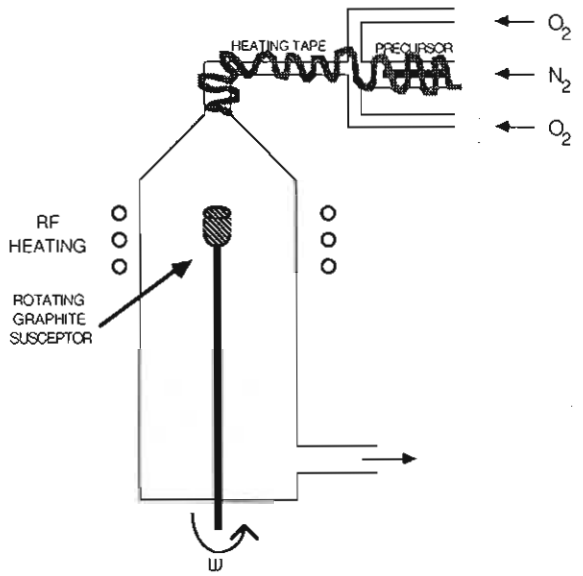

Figure 1. Diagram of the reactor used for chemical vapor deposition under atmospheric pressure.

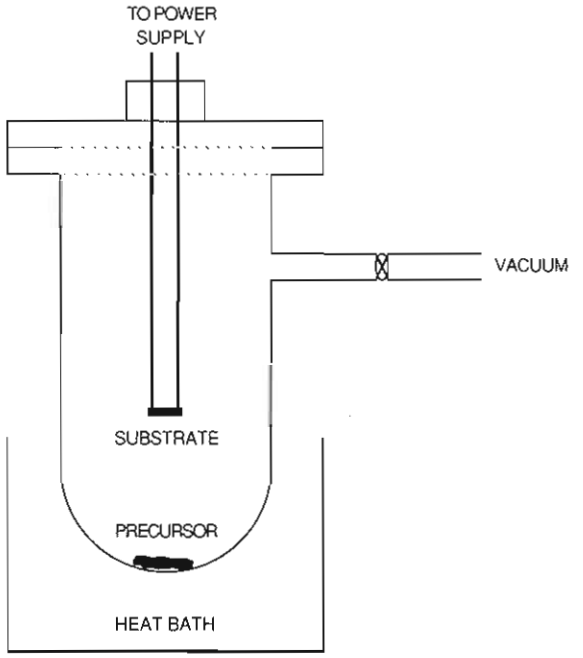

Figure 2. Diagram of the reactor used for chemical vapor deposition under vacuum.

of Ca, Sr, and Ba, as well as a full characterization of the complexes.

Experimental Section

General Comments. All solvents were distilled from sodium benzophenone ketyl before use. Hexafluoroacetylacetone and trifluoroacetylacetone were used as received from Kodak Laboratory and Research Products. Calcium, strontium, and barium chips were obtained from Alfa. NMR spectra were recorded on a JEOL FX-60Q spectrometer using sealed 5-mm tubes containing a C_6D_6 solution of the complex spiked with several drops of THF to improve solubility. Either an internal (for $Ba[HFA]_2$) or an external (for all others) C_6D_6 solution of $CFCl_3$ (δ 0.0, positive values downfield) was used as the ^{19}F reference. Proton spectra were referenced to TMS by using the residual C_6D_5H peak (δ 7.15). Infrared spectra were recorded on a Perkin-Elmer 1430 ratio recording infrared spectrophotometer using a Nujol mull between KBr plates. Sublimation points were determined at $<10^{-5}$ Torr. The mass spectra of the solids were recorded on a Finnigan-MAT TSQ-70 spectrometer at 70 eV, and the mass spectra of the volatile decomposition products were recorded on a CVC MA-2 instrument at 70 eV. Elemental analyses were performed by E+R Microanalytical Laboratory Inc., 96-34 Corona Ave., Corona, NY 11368. Thickness measurements were obtained on a Sloan Dektak 900051 profilometer, and X-ray diffraction spectra were obtained on a Philips APD 3520 powder diffractometer equipped with a Huber horizontal goniometer and a Cu Kα radiation tube. Scanning electron microscopy (SEM) photographs were obtained on an ISI-SS40 instrument, and the Nomarski photograph was obtained on a Nikkon Optiphot microscope.

CVD Experiments. Silicon wafers (with a nominal thickness of 0.4 mm) were cut into pieces between 5 and 15 mm on each side. The pieces were cleaned with detergent, deionized water, acetone, isopropyl alcohol, and boiling trichloroethylene. Atmospheric pressure growths were conducted in the apparatus illustrated in Figure 1. The piece of cleaned silicon was placed, polished side up, on the graphite susceptor, and a small area was masked off with another piece of silicon (~2–5 mm on each side), polished side down. A tube containing the precursor was attached to the reactor and to the nitrogen source. Brief exposure of the precursor to the air occurred during this operation. The susceptor was heated inductively, and the temperature of the precursor (monitored by an Omega 199A digital thermocouple thermometer) was slowly increased until deposition proceeded at a reasonable rate. After completion of the run, the rf generator was turned off when the temperature of the precursor tube was at least 100 °C below its temperature during deposition.

The deposition under vacuum was performed in the apparatus illustrated in Figure 2. The piece of cleaned silicon (polished side down) was secured by two Mo clips. In the Dri-lab, the precursor was loaded and the Conflat UHV flange was tightened. The system was then evacuated to 10^{-5} Torr, and the silicon was resistively heated by using a Systron-Donner Model HR160-3C DC power supply. The temperature of the silicon was estimated by its color since a thermocouple touching the top side appeared to give an irreproducible reading 100–200 °C below its true temperature. Heat was then applied to approximately the lower 5 cm of the apparatus by using an "air bath", which consisted of a 48 mm i.d. × 125 mm long Pyrex tube, wrapped in heating tape and Pyrex cloth, controlled with a Variac instrument. Typically, the temperature applied to the apparatus was less than that normally required for sublimation, as the heat radiated from the silicon was absorbed by the precursor. The tube was allowed to cool before the current to the silicon was turned off.

Auger Electron Spectroscopy. The elemental constituents of the films were determined by Auger electron spectroscopy (AES). The AES spectra were taken with a cylindrical mirror analyzer (Physical Electronics Industries Model 10-155) in a standard vacuum system with a base pressure of 2×10^{-10} Torr. The primary electron energy was 3 keV, and the current density was ~4 mA/cm^2. The AES spectra were recorded in the first-derivative mode with a peak to peak modulation of 1 eV.

An AES spectrum of an as-mounted film was recorded to determine how much adventitious carbon (usually several monolayers or less) was on the film surface. Subsequent Ar^+ sputtering (typically 5×10^{-5} Torr, 700 eV, ~18 μA) removed this carbon. The sputtering times varied from 60 to 120 s, depending on the amount of carbon present.

Example Synthesis: Ba[HFA]$_2$. H[HFA] (2.78 g, 13.3 mmol) was condensed (at −196 °C) onto Ba chips (2.5 mmol) in one side of an H-tube, which was equipped with a stirbar, Kontes K-826510 valves, and a fine frit in the tube connecting each side. A vigorous, exothermic reaction was observed initially along with the rather sudden appearance of a yellow-orange color. The reaction rate slowed appreciably with the precipitation of a white powder. After the mixture was stirred at ambient temperature for 1 day and heated to 40–55 °C for several hours, most of the Ba was consumed. Measurement of the noncondensable gases (presumably H_2) indicated that the reaction proceeded to approximately 60% completion. The solid product was washed with excess H[HFA], which removed most of the orange byproduct. After removal of all volatiles, the off-white solid (0.47 g) remaining on the frit was dissolved in ether, the solution was filtered, and the filtrate was evaporated and dried in vacuo (60 °C, 3 h), leaving an off-white solid. Anal. Calcd (found) for $BaC_{10}F_{12}H_2O_4$: C, 21.8 (21.97); H, 0.59 (0.37); F, 41.3 (41.18); Ba, 24.9 (24.76). NMR: ^1H, δ 6.12; ^{19}F, δ −77.3. IR: 1660 (m, br), 1560 (m), 1535 (s), 1490 (vs, br), 1265 (s), 1205 (s, br), 1160 (vs, br), 805 (m), 745 (w), 670 (m), 585 (m, br) cm^{-1}. Mp: not melting, >210 °C dec. Sublimation point: 205–220 °C.

All subsequent syntheses of M[HFA]$_2$ and M[TFA]$_2$ complexes were done in a similar manner except that THF was used instead of ether in the purification step for the TFA complexes.

Sr[HFA]$_2$: reactants Sr (0.59 g, 6.7 mmol) and H[HFA] (10.44 g, 50 mmol); mixture at room temperature for 12 h and 45–55 °C for 1 day; product dried at 60 °C, 12 h; yield: 1.74 g (51%) of a light yellow solid. Anal. Calcd (found) for $SrC_{10}F_{12}H_2O_4$: C, 23.94 (24.10); H, 0.40 (0.66); F, 45.44 (45.69). NMR: ^1H, δ 6.22; ^{19}F, δ −76.7. IR: 1680 (m), 1660 (s), 1610 (m), 1580 (s), 1560 (m), 1540 (s), 1510 (m), 1340 (m), 1270 (s, br), 1150 (vs, br), 1070 (s), 945 (w), 805 (vs), 770 (w), 745 (m), 740 (w), 675 (s), 665 (s), 590 (m), 530 (w) cm^{-1}. Mp: 220–275 °C dec. Sublimation point: 180–190 °C.

Ca[HFA]$_2$: reactants Ca (0.26 g, 6.5 mmol) and H[HFA] (6.94 g, 50.2 mmol); mixture at room temperature for 5 days and 60 °C for 1 day; product dried at 60 °C, 8 h; yield 1.39 g (47%) of a slightly yellow powder. Anal. Calcd (found) for $CaC_{10}F_{12}H_2O_4$: C, 26.45 (26.62); H, 0.44 (0.60); F, 50.20 (50.05). NMR: ^{1}H, δ 6.23; ^{19}F, δ −76.7. IR: 1680 (s), 1660 (s), 1615 (m), 1555 (s), 1535 (s), 1465 (s, br), 1255 (vs, br), 1200 (s, br), 1145 (vs), 1090 (m), 950 (w), 810 (s), 770 (w), 745 (m), 665 (s), 590 (m), 530 (w) cm^{-1}. Mp: 170–230 °C dec. Sublimation point: 130–150 °C.

Ba[TFA]$_2$: reactants Ba (0.56 g, 4.1 mmol) and H[TFA] (5.26 g, 34.1 mmol); mixture at room temperature for 1 day; product dried at 100 °C, 10 h; yield 1.24 g (76%). Anal. Calcd (found) for $BaC_{10}F_6H_8O_4$: C, 27.08 (27.27); H, 1.82 (1.90); F, 25.70 (25.93). NMR: ^{1}H, δ 1.87 (Me), 5.61 (C–H); ^{19}F, δ −74.8. IR: 1635 (vs), 1530 (m, br), 1280 (s, br), 1230 (w, br), 1185 (m, br), 1135 (m, br), 850 (m), 775 (w), 730 (m), 555 (m) cm^{-1}. Mp: 170–235 °C dec. Sublimation point: 205–215 °C.

Sr[TFA]$_2$: reactants Sr (0.37 g, 4.2 mmol) and H[TFA] (4.15 g, 26.9 mmol); mixture at room temperature 1 day and 40–50 °C 1 day; product dried at 100 °C, 4 h; yield 0.48 g (29%) of an off-white powder. Anal. Calcd (found) for $SrC_{10}F_6H_8O_4$: C, 30.50 (30.50); H, 2.05 (2.11); F, 28.95 (28.93). NMR: ^{1}H, δ 1.85 (Me), 5.67 (C–H), ^{19}F, δ −74.8. IR: 1670 (s), 1630 (vs), 1560–1540 (s), 1280 (vs, br), 1245 (m), 1230 (m), 1180 (m, br), 1120 (s, br), 1020 (w), 1000 (w), 940 (w), 925 (m), 855 (m), 785 (m), 560 (m) cm^{-1}. Mp: 160–230 °C dec. Sublimation point: 200–225 °C.

Ca[TFA]$_2$: reactants Ca (0.50 g, 12.5 mmol) and H[TFA] (14.15 g, 91.8 mmol); mixture at room temperature for 9 days; yellow impurities removed by an ether wash (instead of H[TFA]); yield 3.45 g (79%) of a pale yellow solid. Anal. Calcd (found) for $CaC_{10}F_6H_8O_4$: C, 34.69 (34.54); H, 2.33 (2.16); F, 32.92 (32.61). NMR: ^{1}H, δ 1.80 (Me), 5.69 (C–H); ^{19}F, δ −75.6. IR: 1680 (m), 1670 (m), 1640 (s), 1560 (m), 1530 (m), 1505 (m), 1285 (vs), 1235 (m), 1225 (m), 1185 (m), 1140 (s), 1125 (m), 1000 (w), 955 (w), 940 (w), 860 (m), 790 (w), 730 (w), 570 (m) cm^{-1}. Mp: 170–255 °C dec. Sublimation point: 190–200 °C.

Results and Discussion

All the M[HFA]$_2$ and M[TFA]$_2$ complexes were prepared from the reaction of excess fluorinated acetylacetone with the metal. The reactions would start very vigorously but would slow down when product started to precipitate. An orange byproduct also formed during these reactions and was most prevalent in those that were allowed to rise above room temperature. This orange material had a very complex ^{19}F NMR spectrum and would appear to be from decomposition of the ligand. This substance was easily removed by repeatedly washing the product with excess ligand. All the HFA salts were readily soluble in both ether and THF, but the TFA complexes were soluble only in THF. Any bound ether or THF was easily removed by heating under vacuum.

The HFA complexes were more volatile than the TFA complexes, and as expected, the volatility of the complexes decreased in the order Ca > Sr > Ba. It is well-known that increasing the ionic radii of the metal ions in a given series of complexes decreases their volatility. Several factors are involved, but the decrease in ligand shielding of the metal and the increases in polarizability and potential coordination number of the metal are primary causes.[13-15] All of the complexes decompose when heated between 170 and 260 °C, which is within the range reported for other acetylacetonates.[16,17] The volatile product from those decompositions was primarily free ligand as determined by mass spectra. A nonvolatile black solid was also formed during decomposition.

Mass Spectra. The peaks at m/e 69 (CF_3^+), 139 ($F_3CC(O)CH_2C(O)^+$), and 208 (H[HFA]$^+$) from the loss and fragmentation of the HFA ligand were prominant in the mass spectra of the M[HFA]$_2$ complexes. It is unknown whether the ligand was lost during heating or from electron impact since free ligand is a thermal decomposition product of these complexes (complexes sublime with decomposition). The mass spectra of the TFA compounds also contain fragments of the ligand, with the most prominent peaks occurring at m/e 85 ($H_3CC(O)CH_2C(O)^+$) and 154 (H[TFA]$^+$).

A number of intense high-mass peaks, including ML^+, $M_2F_2L^+$, $M_2L_2F^+$, and $M_2L_3^+$, appeared in the fragmentation patterns of all the HFA complexes. The $M_2L_3^+$ peak was very prominent in all the spectra and was the base peak for Ca[HFA]$_2$. In addition, $M_3L_4F^+$ or $M_3L_4F^+ - H$ and $M_3L_5^+$ were also seen in the spectra of Ca[HFA]$_2$ and Sr[HFA]$_2$. Molecular ion peaks, $(ML_2)_n$, were not observed. The pattern of fragmentation is consistent with observations made on other group II acetylacetonate complexes[18,19] such as Ca[TPM]$_2$,[20] M[TMHD]$_2$,[15] and Mg[HFA]$_2$·xH$_2$O.[21]

The high-mass peaks correspond to different fragments for different complexes. For Ca[HFA]$_2$ a peak at m/e 1517 ($Ca_6L_6OF^+$) was the highest mass of significant (5%) intensity, although a higher peak at m/e 1952.5 corresponding to either $Ca_7L_8F^+ - 2H$ or $Ca_7L_8O^+$ was also observed. The highest mass peak for Sr[HFA]$_2$ was at m/e 1859, corresponding to $Sr_7L_6^+$. The highest mass peak for Ba[HFA]$_2$ was $Ba_2L_3^+$ at m/e 897. In contrast, the TFA complexes showed little in the way of high-mass peaks, with no peaks >1% beyond m/e 539 ($Ca_2L_3^+$) for Ca[TFA]$_2$, m/e 400 in Sr[TFA]$_2$, and m/e 220 in Ba[TFA]$_2$. Scale expansion of the high-mass regions did show very small peaks, some of which were identified as follows: $Ca_2L_4F_2^+ - Me$ (m/e 751), $Ca_3L_5^+$ (885), $Ca_4L_5F_2^+$ (963), and $Ca_4L_6F^+$ (1097);

Table I. Mass Spectral Data (m/e) of HFA and TFA Complexes[a]

	Ca[HFA]$_2$	Sr[HFA]$_2$	Ba[HFA]$_2$
CF_3^+	80	99	100
H[HFA]$^+ - CF_3$	71	100	98
H[HFA]$^+$	16	57	61
ML^+	44*	49*	47
$M_2LF_2^+$	64*	69*	39*
$M_2L_2F^+$	68*	86	40*
$M_2L_3^+$	100*	76	24*
$M_3L_2F_3^+$	20*	37*	1
$M_3L_4F^+$	37	31	
$M_3L_4F^+ - H$		58	
$M_3L_5^+$	51*	6	
$M_4L_5F_2^+$	5 (−H)	7	
$M_4L_6F^+$	44	56*	
$M_6L_6OF^+$	7		
$M_7L_6^+ - O$		26*	
$M_7L_6^+$		11	
$M_7L_8F^+ - 2H$ (?) or $M_7L_8O^+$ (?)	1		

	Ca[TFA]$_2$	Sr[TFA]$_2$	Ba[TFA]$_2$
CF_3^+	58	72	61
H[TFA]$^+ - CF_3$	100	100	100
H[TFA]$^+$	56	72	54
ML^+	2	1	
$M_2LF_2^+$	5	0.6	0.04
$M_2L_2F^+$	4*	0.1	0.03
$M_2L_3^+$	6*	0.09	0.02
$M_2L_4F_2^+ - CH_3$	0.18		
$M_3L_3F_2^+$	0.30	0.01	
$M_3L_4F^+$	0.80*	0.03	
$M_3L_5^+$	0.10		
$M_4L_5F_2^+$	0.03		
$M_4L_6F^+$	0.60*	0.01	

[a] An asterisk indicates a good match with the computed isotope pattern (see text).

(13) Eisentraut, K. J.; Sievers, R. E. *J. Am. Chem. Soc.* **1965**, *87*(22), 5254.
(14) Sicre, J. E.; Dubois, J. T.; Eisentraut, K. J.; Sievers, R. E. *J. Am. Chem. Soc.* **1969**, *91*, 3476.
(15) Schwarberg, J. E.; Sievers, R. E.; Moshier, R. W. *Anal. Chem.* **1970**, *42*(19), 1828.
(16) Van Hoene, J.; Charles, R. G.; Hickam, W. M. *J. Am. Chem. Soc.* **1958**, *62*, 1098.
(17) Domrachev, G. A.; Shitova, E. V.; Vodzinskii, V. Yu.; Suvorova, O. N.; Varyukhin, V. A.; Nesterov, B. A. *Dokl. Akad. Nauk SSSR* **1976**, *226*(5), 1080.
(18) MacDonald, C. G.; Shannon, J. S. *Aust. J. Chem.* **1966**, *19*, 1545.
(19) Reichert, C.; Bancroft, G. M.; Westmore, J. B. *Can. J. Chem.* **1970**, *48*, 1362.
(20) Belchev, R.; Crante, C. R.; Majer, J. R.; Stephen, W. I.; Uden, P. C. *Anal. Chim. Acta* **1972**, *60*, 109.
(21) Janghorbani, M.; Welz, I.; Starke, K. *J. Inorg. Nucl. Chem.* **1976**, *38*, 41.

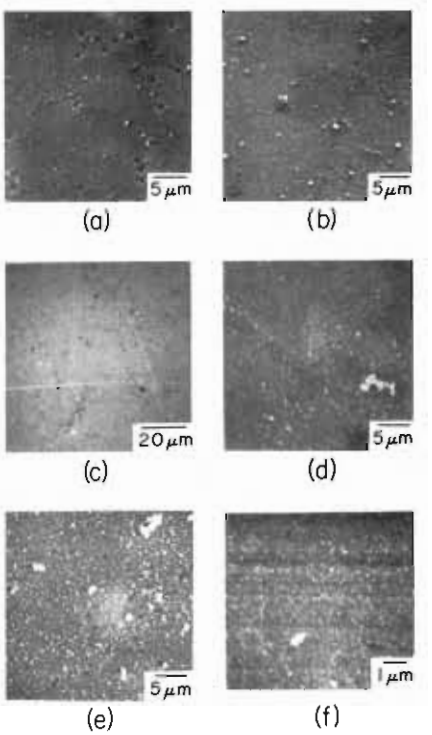

Figure 3. Scanning electron microscopy and Nomarski photographs of films: (a) $Ca[HFA]_2$ (N_2 and O_2), 3000×; (b) $Ca[HFA]_2$ (N_2), 2600×; (c) $Ca[HFA]_2$ (vacuum), 1000× (Nomarski photograph); (d) $Ca[TFA]_2$, (N_2 and O_2), 2800×; (e) $Sr[HFA]_2$ (N_2 and O_2), 2800×; (f) $Ba[HFA]_2$ (N_2 and O_2), 10000×.

SrL_2O^+ (*m/e* 410), $Sr_2L_2^+$ (635), $Sr_3L_3F_2^+$ (761), $Sr_3L_4F^+$ (895), and $Sr_4L_6F^+$ (1289); $Ba_2L_2F^+$ (*m/e* 601) and $Ba_2L_3^+$ (735). The low intensities of these high-mass peaks can be accounted for by a majority of the sample decomposing rather than being transported in the spectrometer. The intensities of the mass peaks are listed in Table I. Isotope patterns of all the listed metal-containing peaks were reasonably consistent with those computed from natural abundances. Those isotope patterns that show a particularly good match are so indicated in Table I.

CVD Experiments. Four of the complexes, $Ca[HFA]_2$, $Sr[HFA]_2$, $Ba[HFA]_2$, and $Ca[TFA]_2$, were successfully used as precursors in CVD experiments, in which films were grown on a heated silicon substrate. The two other TFA complexes were not volatile enough for transport at atmospheric pressure and were not used.

For film growth at atmospheric pressure, the temperature of the inductively heated susceptor was between 500 and 525 °C, and a steady flow of nitrogen transported the precursor vapors into the reactor. With enough oxygen also flowing into the reactor to provide an oxygen-rich atmosphere, metal fluoride films containing small (<5%) amounts of carbon and oxygen were formed. X-ray diffraction patterns of the films grown from each of the precursors under an oxidizing atmosphere indicated the presence of metal fluorides. The X-ray reflections from the BaF_2 film were strong ($I_1 \approx 2\%$ of $d = 1.36$ Å Si peak), indicating high crystallinity, but those from the other films were weak ($I_1 \approx 0.03$–0.2% of Si $d = 1.36$ Å peak). Recent reports[3,8,9] have detailed the use of $Ba[HFA]_2$ and other fluorinated Ba chelate compounds for the CVD of Y–Ba–Cu–O superconductors. Typically, deposition under dry O_2 resulted in fluoride films, and the fluorides were converted wholly or partly to the oxides through the use of water vapor[8,9] or high-temperature annealing.[3] No attempt was made to convert any of our fluoride films to the oxides. A film grown from $Ca[HFA]_2$ (with nitrogen flow only) contained substantial (~50%) carbon as determined by Auger analysis. A nearly identical result occurred when a film was grown from $Ca[HFA]_2$ under vacuum, and thus an oxidant appears necessary to remove carbon during deposition. Other workers have reported a similar result when $Al[HFA]_3$ or $Be[HFA]_2$ was used.[10,22] The films were relatively fine-grained with few surface features as seen in the SEM photographs (Figure 3). Complete experimental conditions for each film growth and the X-ray diffraction and thickness data on each film are listed in Tables II and III, respectively.

Table II. Deposition Conditions for Films

Depositions at Atmospheric Presure

precursor	temp, °C inlet	temp, °C substrate	flow rates, L min^{-1} N_2	flow rates, L min^{-1} O_2	time	precursor quantity, g
$Ca[HFA]_2$	180–185	475–500	0.2	1	2 h	0.1
$Ca[HFA]_2$	185–190	525	0.6	0	45 min	0.13
$Sr[HFA]_2$	220–225	525	0.25	1	2 h	0.1
$Ba[HFA]_2$	240–255	525	0.25	1	1.5 h	0.08
$Ca[TFA]_2$	240–250	525	0.25	1	2 h	0.1

Deposition under Vacuum

precursor	temp, °C bath	temp, °C substrate	time, min	precursor quantity, g
$Ca[HFA]_2$	80–120	500–600	20	0.06

Table III. X-ray Diffraction and Thickness Data for the Films

precursors; gases; thickness, Å	2θ, deg	*d*, Å exptl	*d*, Å lit.[26]	*I*, % exptl	*I*, % lit.[26]
$Ca[HFA]_2$; N_2, O_2; 4900	28.3	3.15	3.153	40	94
	47	1.93	1.931	20	100
	55.7	1.64	1.647	100	35
$Ca[HFA]_2$; N_2 only; 4000	broad, low-intens hump, 13–36°				
$Sr[HFA]_2$; N_2, O_2; 4800	26.41	3.37	3.35	100	100
	43.96	2.06	2.05	70	80
	52.08	1.75	1.75	62	52
$Ba[HFA]_2$; N_2, O_2; 3000	24.71	3.60	3.579	100	100
			2.193		79
			1.870		51
	50.84	1.79	1.79	7	3
$Ca[TFA]_2$; N_2, O_2; 5300	28.12	3.17	3.153	100	94
	46.85	1.94	1.931	57	100
	55.8	1.65	1.647	35	35
$Ca[HFA]_2$; vacuum, 10600	28.4	3.14	3.153		94
	46.4	1.96			
	47.0	1.93	1.931		100
			1.647		35

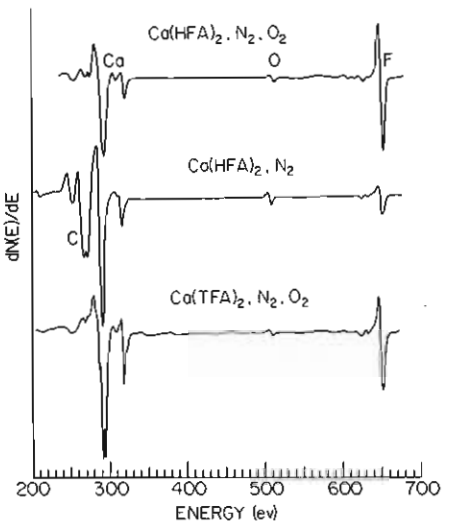

Figure 4. Auger electron spectra of calcium-containing films.

Auger Electron Spectroscopy. Fluorides are sensitive to electron-beam-induced damage resulting from electron-stimulated

(22) Power, J. M.; Sarhangi, A. U.S. Patent 4718929, 1988; *Chem. Abstr.* **1988**, *108*, 117548.

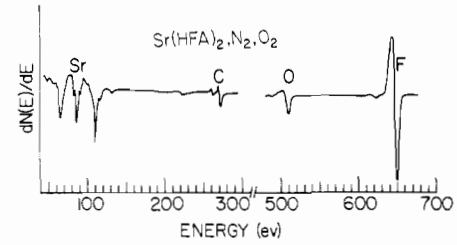

Figure 5. Auger electron spectrum of the SrF_2 film.

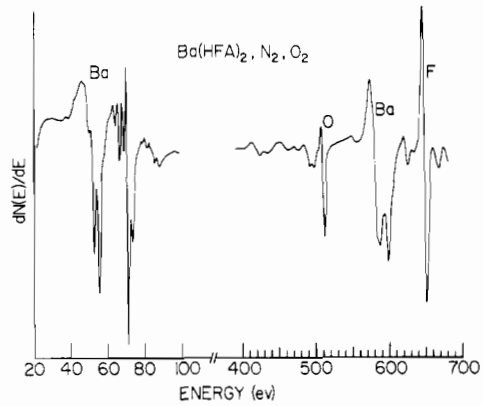

Figure 6. Auger electron spectrum of the BaF_2 film, C peak not shown (see text).

desorption.[23] For the AES spectra of our films, the F peak-to-peak height decreased rapidly with a time constant of tens of seconds. Therefore, before a spectrum was recorded, the sample was moved so that the electron beam impinged onto an unexposed area and the F line was recorded immediately. As a result, the quantitative comparison of the F peak-to-peak height with those of the metals is not meaningful.

Figure 4 shows Auger spectra for films grown from $Ca[HFA]_2$ with and without O_2 and from $Ca[TFA]_2$ with O_2. Although the C and Ca lines overlap, it is apparent that films grown with O_2 have very little C. However, the C content is large in films grown without O_2. All the Ca films contained a substantial amount of F but only several percent of O. Note that the Ca lines at 291 and 294 eV are resolved for the film grown from $Ca[TFA]_2$.

Figure 5 shows an Auger spectrum for a film grown from $Sr[HFA]_2$ with O_2. The dominant peaks are Sr and F, although there are several percent of C and O. The carbon is in the carbidic form.

Figure 6 shows an Auger spectrum from a film grown from $Ba[HFA]_2$ with O_2. The dominant peaks are Ba and F. The line shapes of the Ba lines between 40 and 80 eV indicate that the Ba is mostly elemental.[24] However, the presence of the peak near 68 eV indicates that some of the Ba was oxidized, which is commensurate with the small O line. For a fully oxidized Ba surface,[25] the ratio of the peak-to-peak heights of the Ba (584 eV) line to the O (510 eV) line would be 0.5. The peak-to-peak height of the C line (not shown) was ~4% of that of the Ba (584 eV) line. The C had a carbidic line shape.

Acknowledgment. We thank Mark Ross and John Callahan for their assistance with the mass spectral analysis.

Registry No. $Ba[HFA]_2$, 118131-57-0; $Sr[HFA]_2$, 121012-89-3; $Ca[HFA]_2$, 121012-90-6; $Ba[TFA]_2$, 84653-56-5; $Sr[TFA]_2$, 121012-91-7; $Ca[TFA]_2$, 73592-45-7; BaF_2, 7787-32-8; SrF_2, 7783-48-4; CaF_2, 7789-75-5; Si, 7440-21-3.

(23) Strecker, C. L.; Noddeman, W. E.; Grant, J. T. *J. Appl. Phys.* **1981**, *52*, 6921.
(24) Haas, G. A.; Marian, C. R. K.; Shih, A. *Appl. Surf. Sci.* **1983**, *16*, 125.
(25) Shih, A.; Hor, C.; Haas, G. A. *Appl. Surf. Sci.* **1979**, *2*, 112.
(26) Powder Diffraction File (ASTM Cards); Joint Committee on Powder Diffraction Standards, Swarthmore, PA; Files 4-0864 (CaF_2), 6-0262 (SrF_2), 4-070 (BaF_2).

Contribution from the Department of Chemistry, The University of Calgary, Calgary T2N 1N4, Alberta, Canada

Lewis Base Properties of $1\lambda^5,3\lambda^5$-Diphospha-5-thia-2,4,6-triazines: Crystal and Molecular Structures of $(Ph_4P_2N_3SPh)Me^+CF_3SO_3^-$

Tristram Chivers,* James Fait, and Stephen W. Liblong

Received December 28, 1988

The behavior of $Ph_4P_2N_3SPh$ (**1**) toward Lewis and Brønsted acids has been investigated, and the following adducts have been isolated: $(Ph_4P_2N_3SPh)H^+BF_4^-$ (**5**), $(Ph_4P_2N_3SPh)Me^+CF_3SO_3^-$ (**6**), $Ph_4P_2N_3SPh{\cdot}BF_3$ (**7**), and $Ph_4P_2N_3SPh{\cdot}BCl_3$ (**8**). The ^{31}P NMR spectrum of **6** reveals inequivalent phosphorus atoms, indicating that the methyl group is coordinated to a nitrogen atom between a phosphorus and a sulfur atom of the P_2N_3S ring. An X-ray structural determination has confirmed this assignment. The crystals of **6** are monoclinic and belong to the space group $P2_1/c$, with a = 10.317 (2) Å, b = 22.849 (4) Å, c = 14.104 (3) Å, β = 102.94 (2)°, V = 3241 (1) Å^3, and Z = 4. The final R and R_w values were 0.046 and 0.049, respectively. The P_2N_3S ring in **6** adopts a highly distorted boat conformation. The bond lengths to the coordinated nitrogen are lengthened compared to those of the parent ring system [1.69 vs 1.62 Å for d(S–N) and 1.69 vs 1.62 Å for d(P–N)], and the adjacent S–N and P–N bonds are shortened slightly. By contrast, the ^{31}P NMR spectrum of **5** exhibits a singlet consistent with protonation at the unique nitrogen atom of the P_2N_3S ring. Compounds **7** and **8** display ^{31}P NMR spectra consistent with the formation of both symmetrical and unsymmetrical adducts. The lack of regioispecificity in the formation of adducts between the P_2N_3S ring and Lewis or Brønsted acids is discussed in terms of the electronic structure of the heterocycle.

Introduction

All four members of the series of inorganic heterocycles containing alternating phosphorus or sulfur and nitrogen atoms, **1–4**, are known,[1] and their π-electronic structures have been compared.[2]

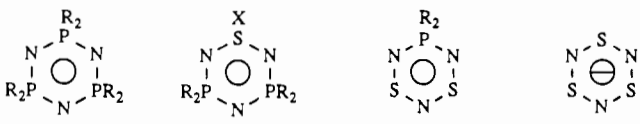

1 **2** **3** **4**

The Lewis base properties of **1**,[3] **3**,[4] and **4**[5] have also been investigated, and the formation of a variety of adducts with Lewis

(1) Chivers, T. *Acc. Chem. Res.* **1984**, *17*, 166.
(2) Burford, N.; Chivers, T.; Hojo, M.; Laidlaw, W. G.; Richardson, J. F.; Trsic, M. *Inorg. Chem.* **1985**, *24*, 709.
(3) Allen, C. W. In *The Chemistry of Inorganic Homo- and Heterocycles*; Haiduc, I., Sowerby, D. B., Eds.; Academic: London, 1987; Vol. 2, p 563.
(4) Chivers, T.; Liblong, S. W.; Richardson, J. F.; Ziegler, T. *Inorg. Chem.* **1988**, *27*, 860.

0020-1669/89/1328-2803$01.50/0